Supplemental information

In silico study on the effects of disulfide bonds in ORF8 of SARS-CoV-2

Yadi Cheng[a] and Xubiao Peng[a,b,*]

a Center for Quantum Technology Research, Key Laboratory of Advanced Optoelectronic Quantum Architecture and Measurements (MOE), School of Physics, Beijing Institute of Technology, Beijing 100081, China

b Beijing Academy of Quantum Information Sciences, Beijing 100193, China E-mail: xubiaopeng@bit.edu.cn
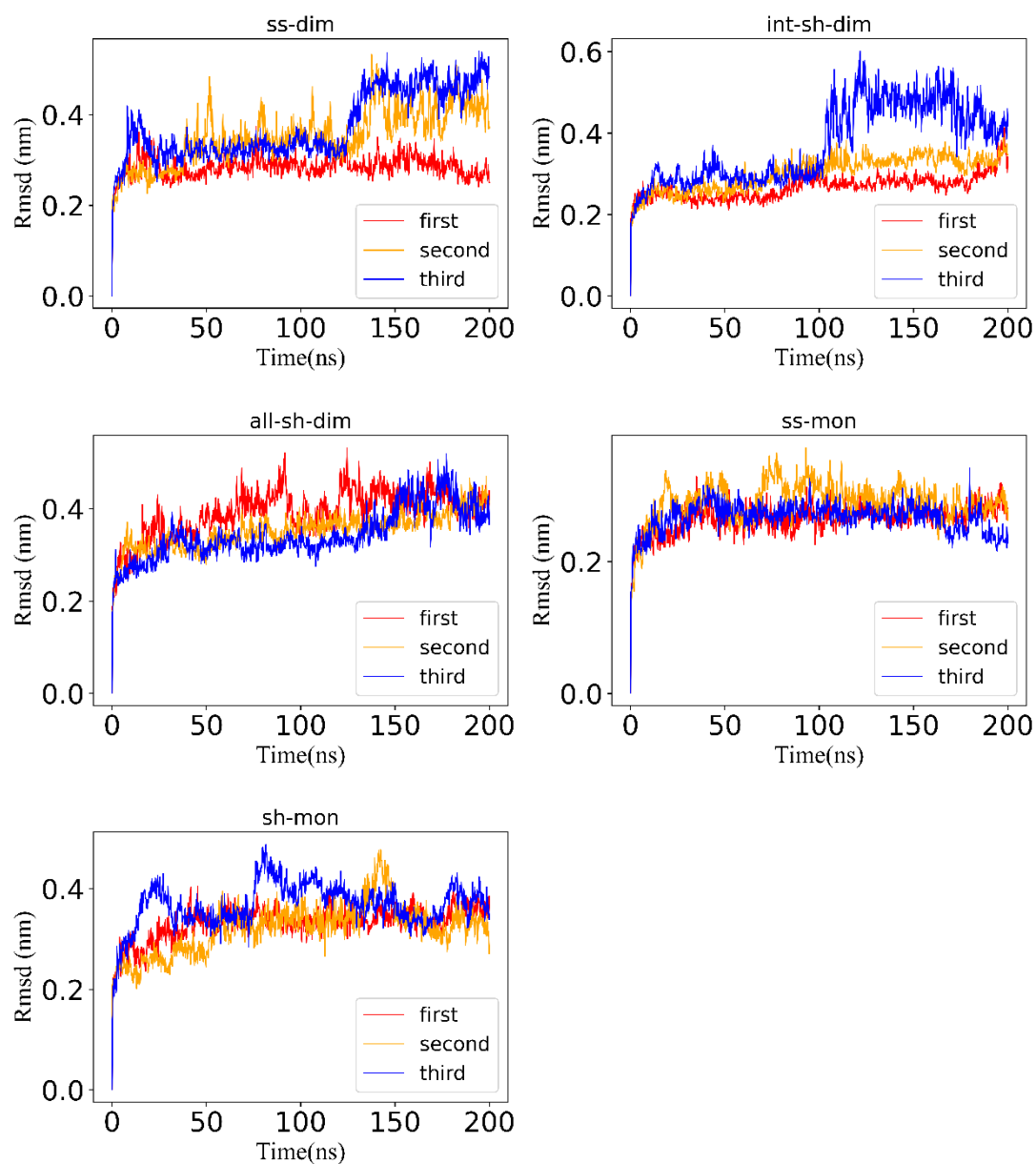
Contents:

Fig. S1 The curves of RMSD evolution for the three replicated MD simulations on five different disulfide bonding states.
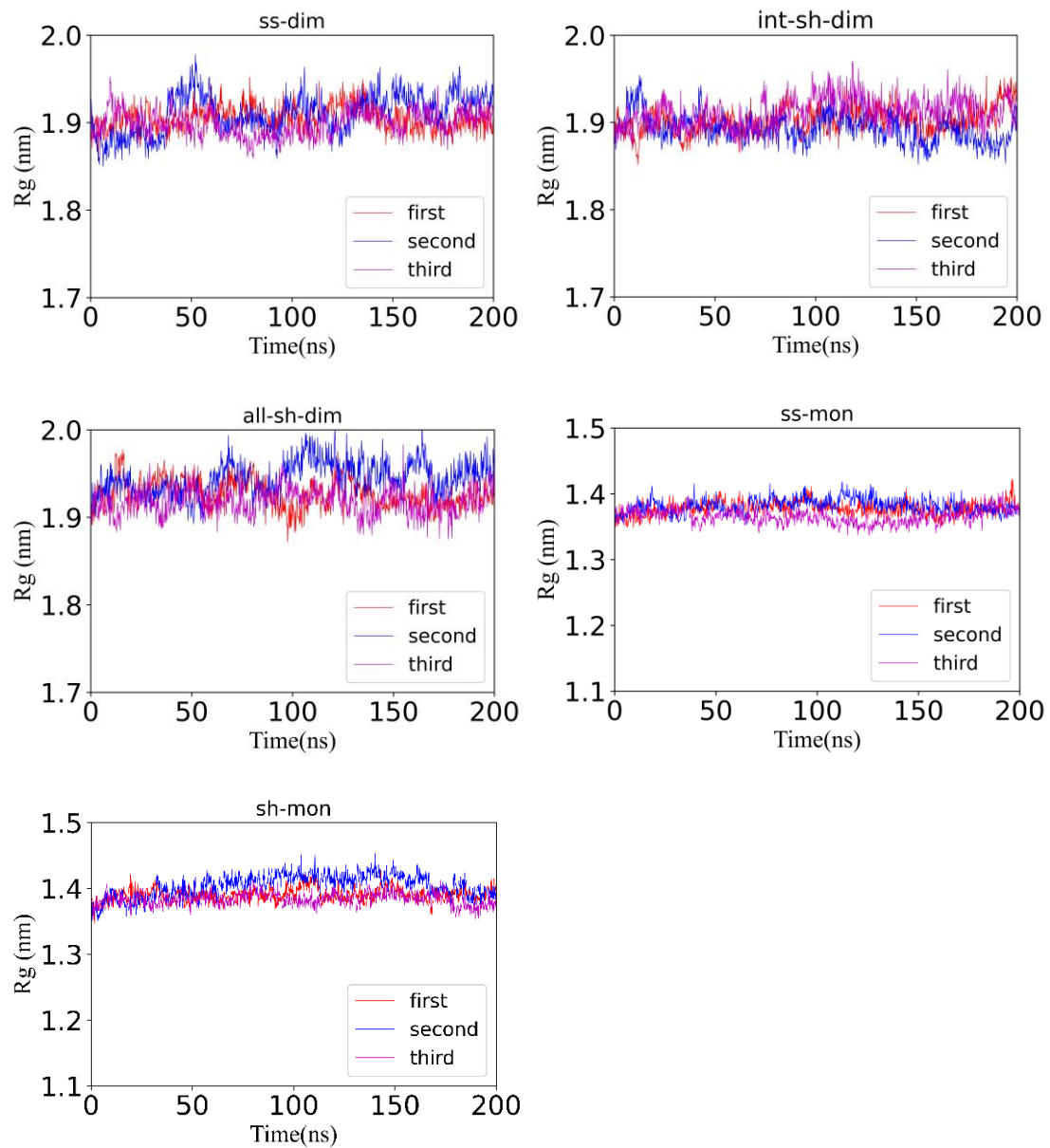
Fig. S2. The Rg curves for the three replicated MD simulations on five different disulfide bonding states.
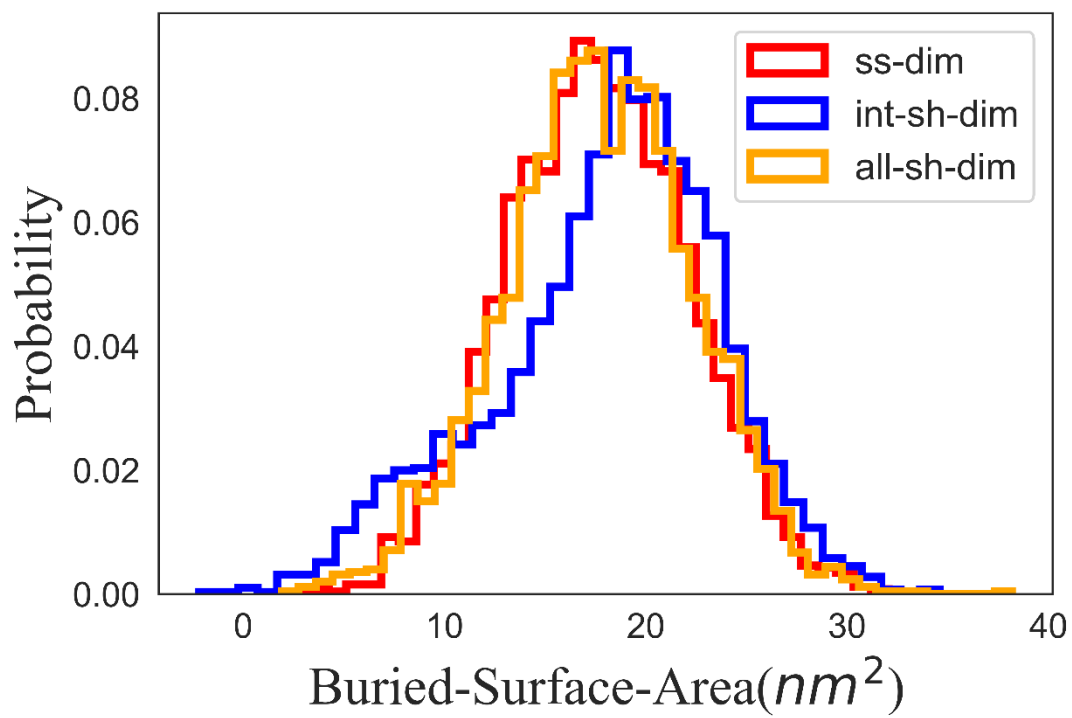
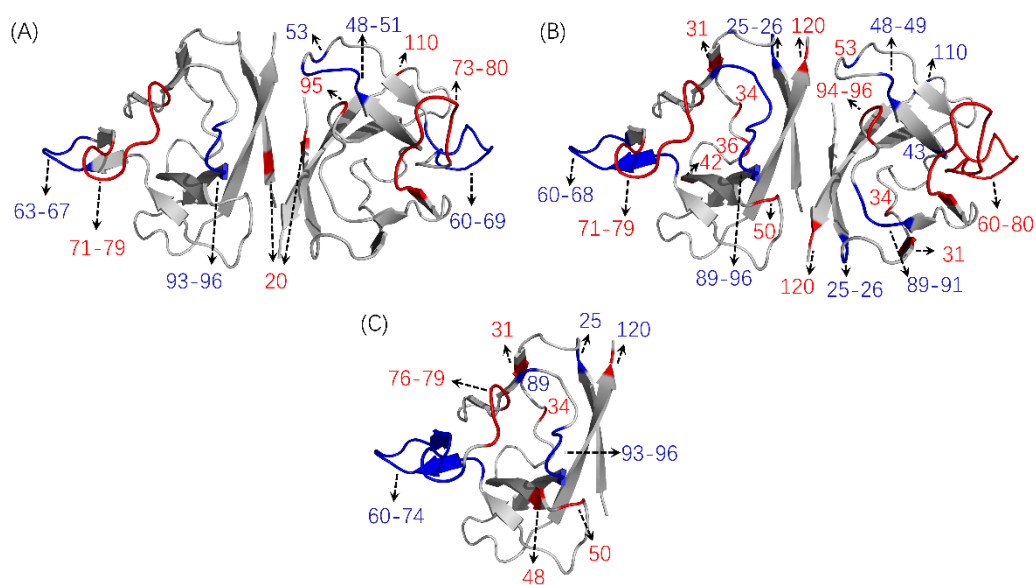Fig. S3. The distributions of the buried surface area for the three dimeric states.

Fig. S4. The locations of the residues that are most affected by different disulfide bonds reduction schemes. (A) interchain disulfide bond reduction in dimer (B) all disulfide bonds reduction in dimer (C) intrachain (all) disulfide bonds reduction in monomer.
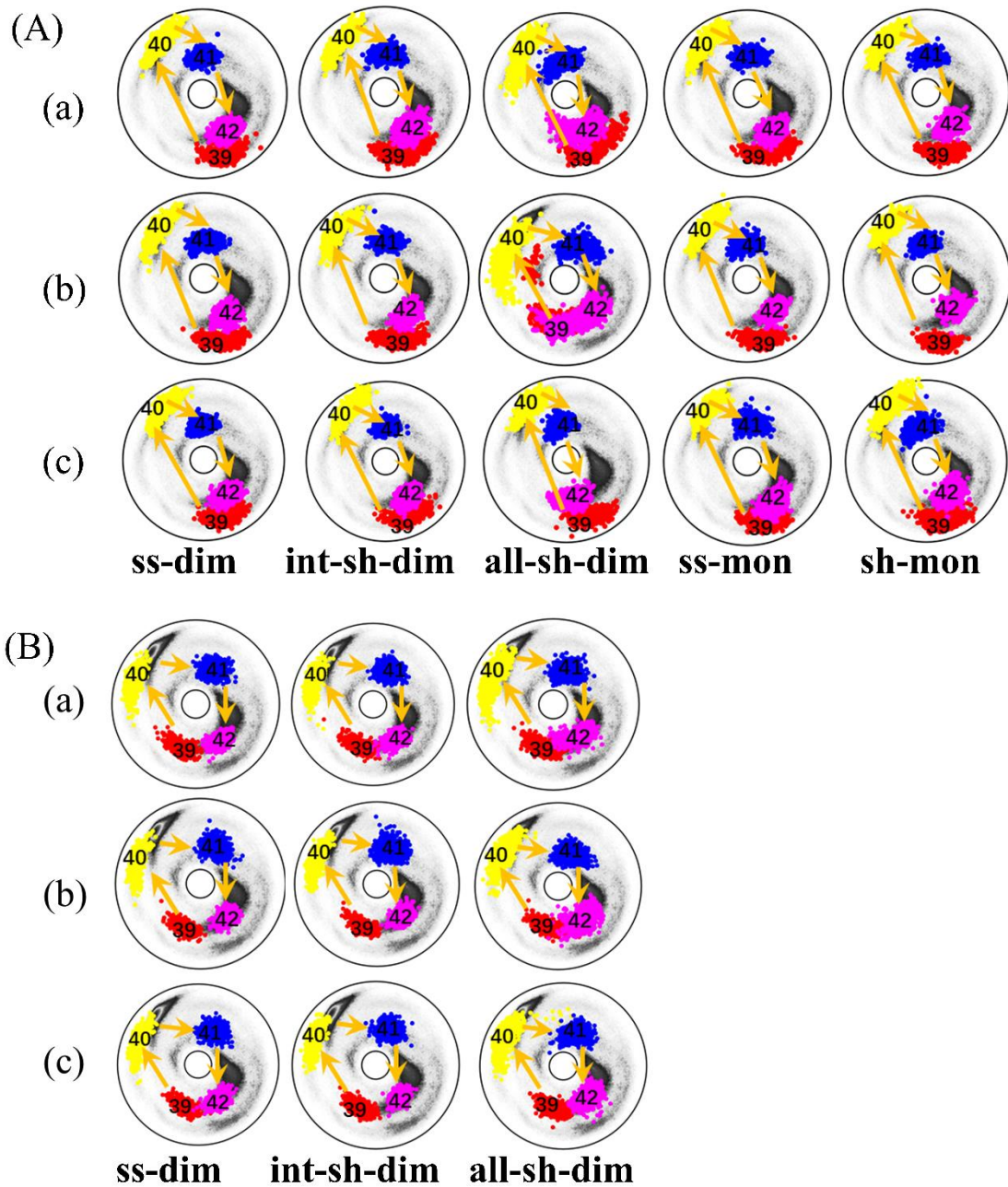
Fig. S5. The distributions of the angle pairs (κ_i, τ_i) with $i \in$ [39, 42] for the segment ^{39}IHFY^{42}. Panel (A) and (B) are for chain A and B, respectively. In each panel, rows (a), (b), and (c) are the results from the first, second and third replicated simulation, respectively.

(A)

(a)

(b)

(c)

ss-dim   **int-sh-dim**   **all-sh-dim**   **ss-mon**   **sh-mon**

(B)

(a)

(b)

(c)

ss-dim   **int-sh-dim**   **all-sh-dim**

Fig. S6. The distributions of the angle pairs (κ_i, τ_i) with $i \in [104, 107]$ for the segment ^{104}FYED^{107}. Panel (A) and (B) are for chain A and B, respectively. In each panel, rows (a), (b), and (c) are the results from the first, second and third replicated simulation, respectively.
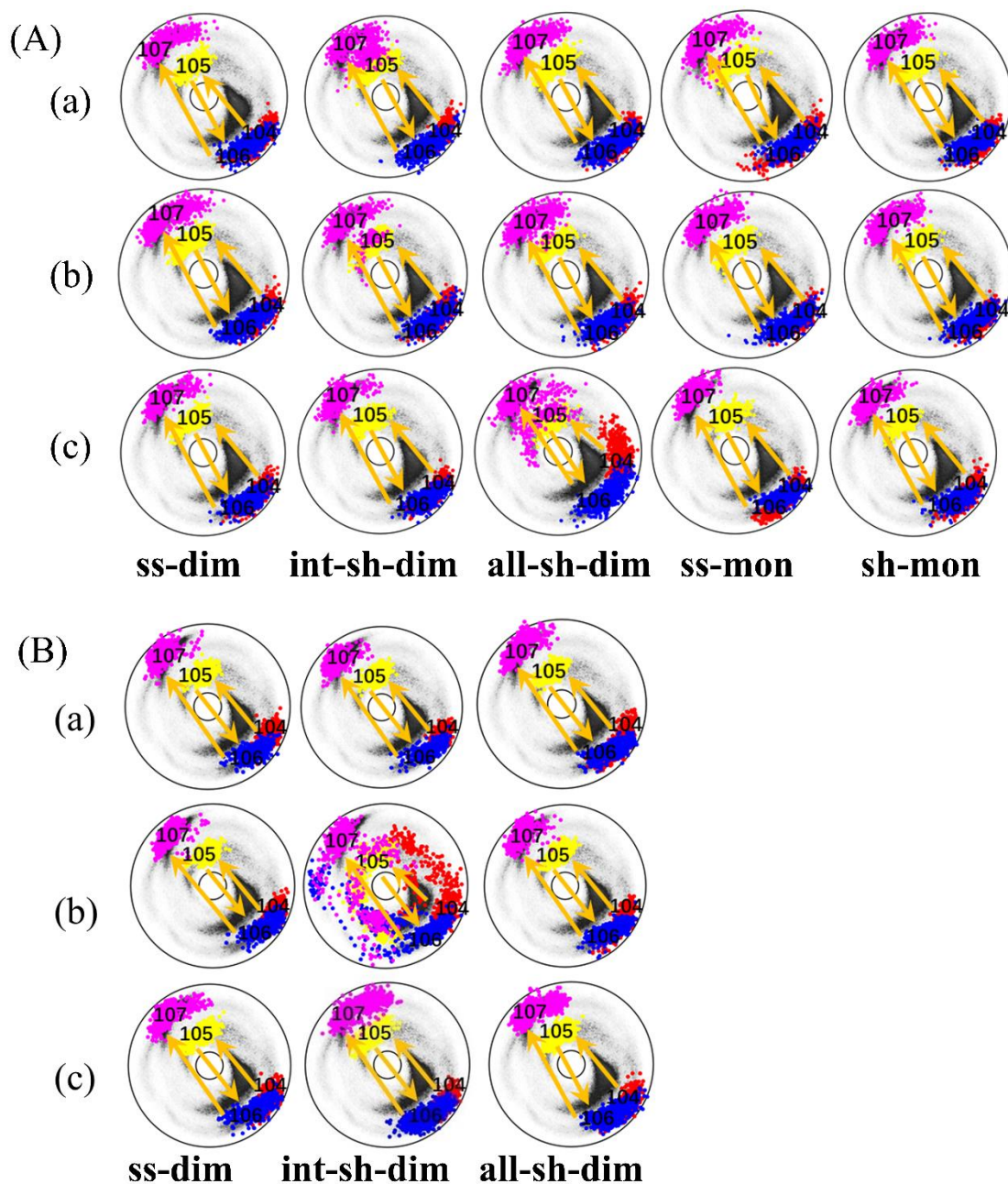
Fig. S7. The distributions of the angle pairs (κ_i, τ_i) with $i \in [110, 112]$ for the segment ^{110}EYH^{112}. Panel (A) and (B) are for chain A and B, respectively. In each panel, rows (a), (b), and (c) are the results from the first, second and third replicated simulation, respectively.
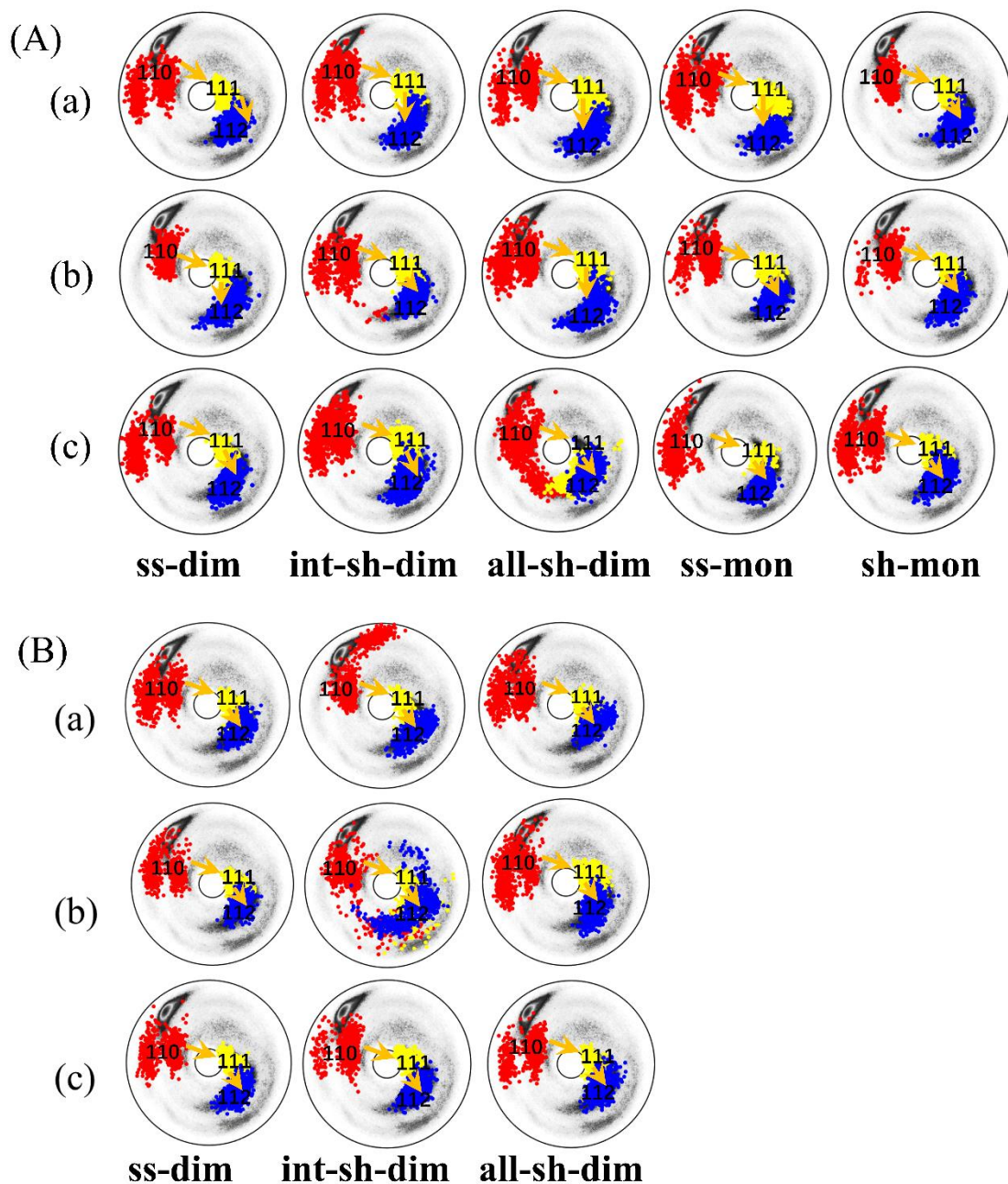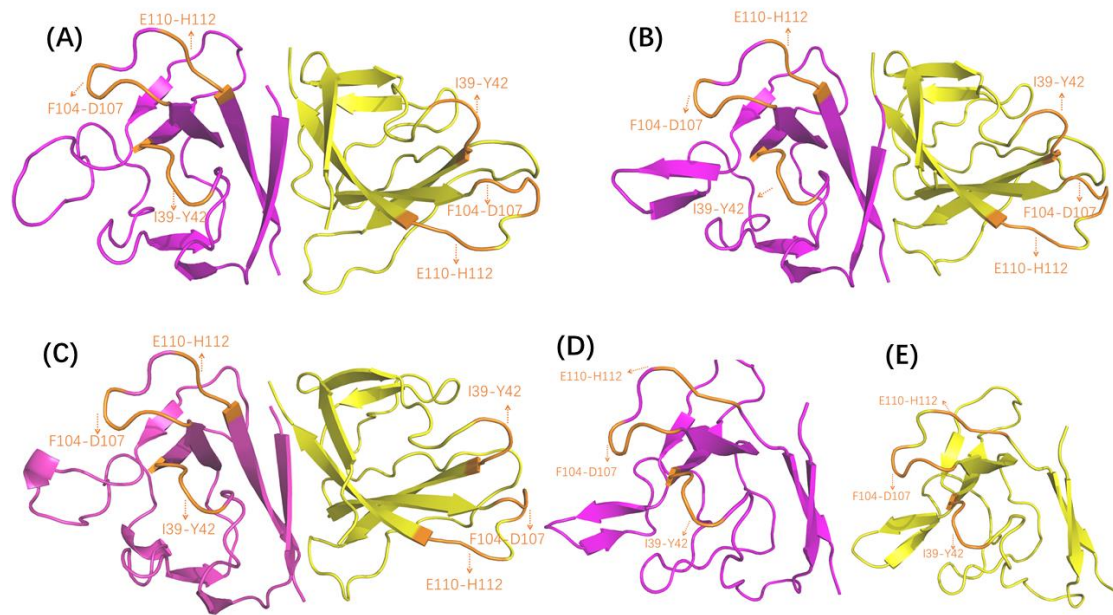
Fig. S8. The location of the three conserved segments relative to disulfide bonds reduction in the representative structures of five states. (A) ss-dim.(B) int-sh-dim.(C) all-sh-dim.(D) ss-mon.(E) sh-mon. In each panel, the chains A and B are colored in magenta and yellow, respectively.
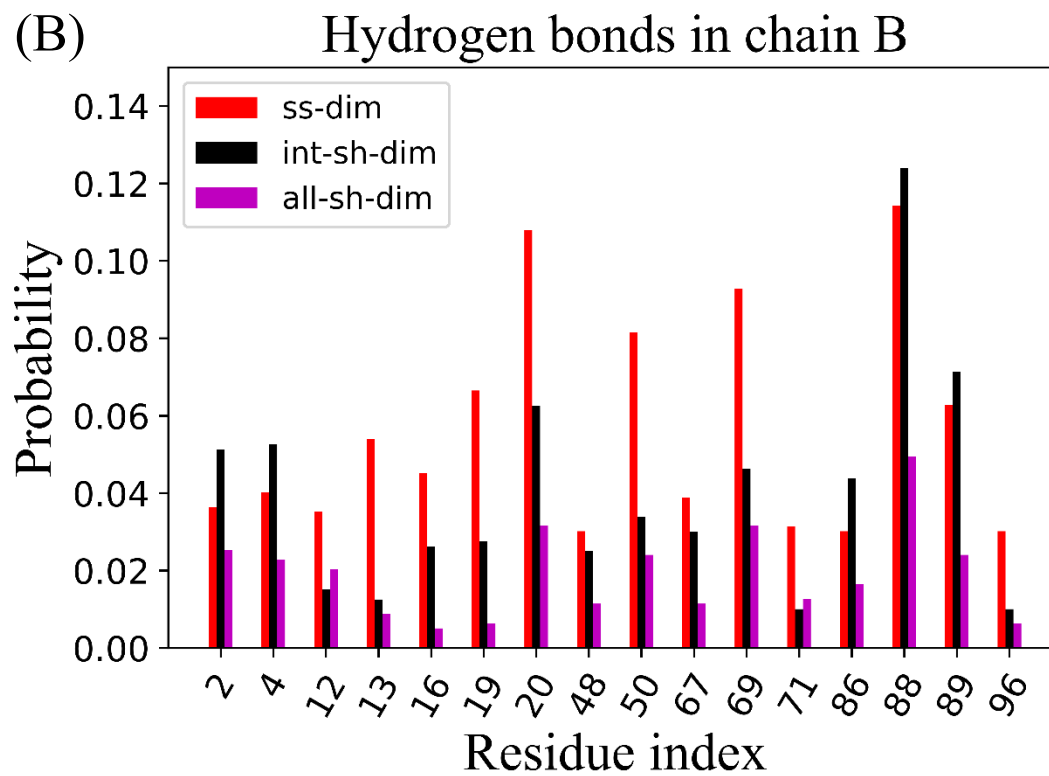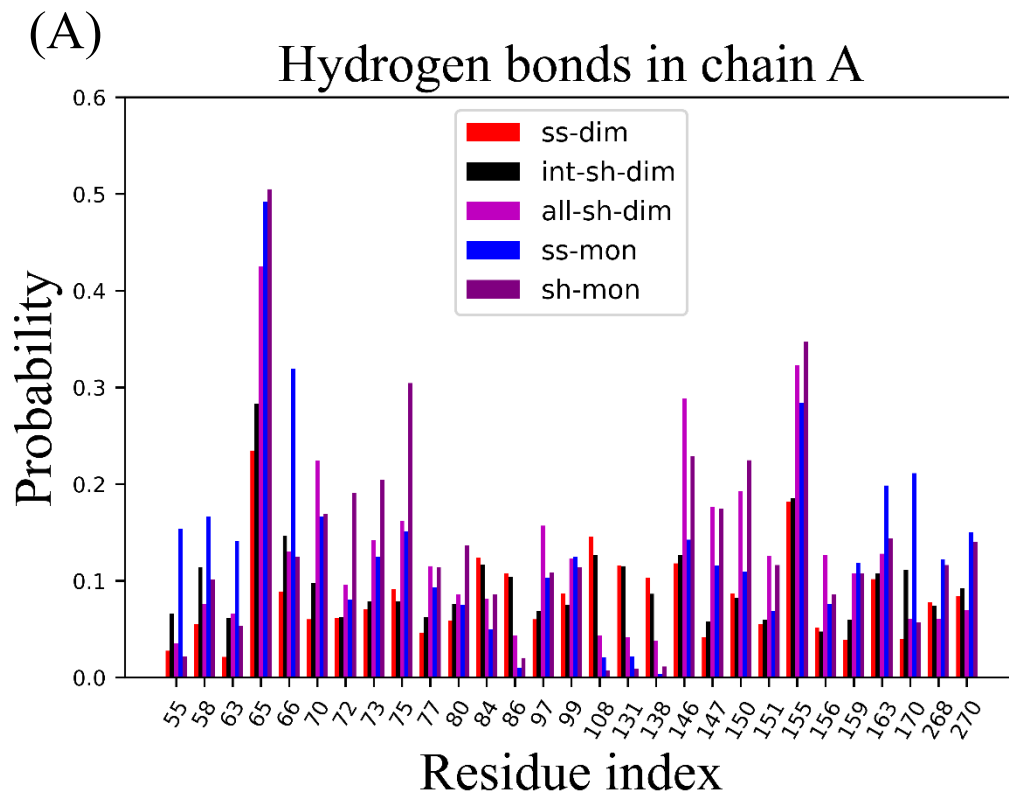
Fig. S9 The distributions of the binding sites on HLA-A forming in hydrogen bonds with ORF8. (A) For chain A of HLA-A (B) For chain B of HLA-A.
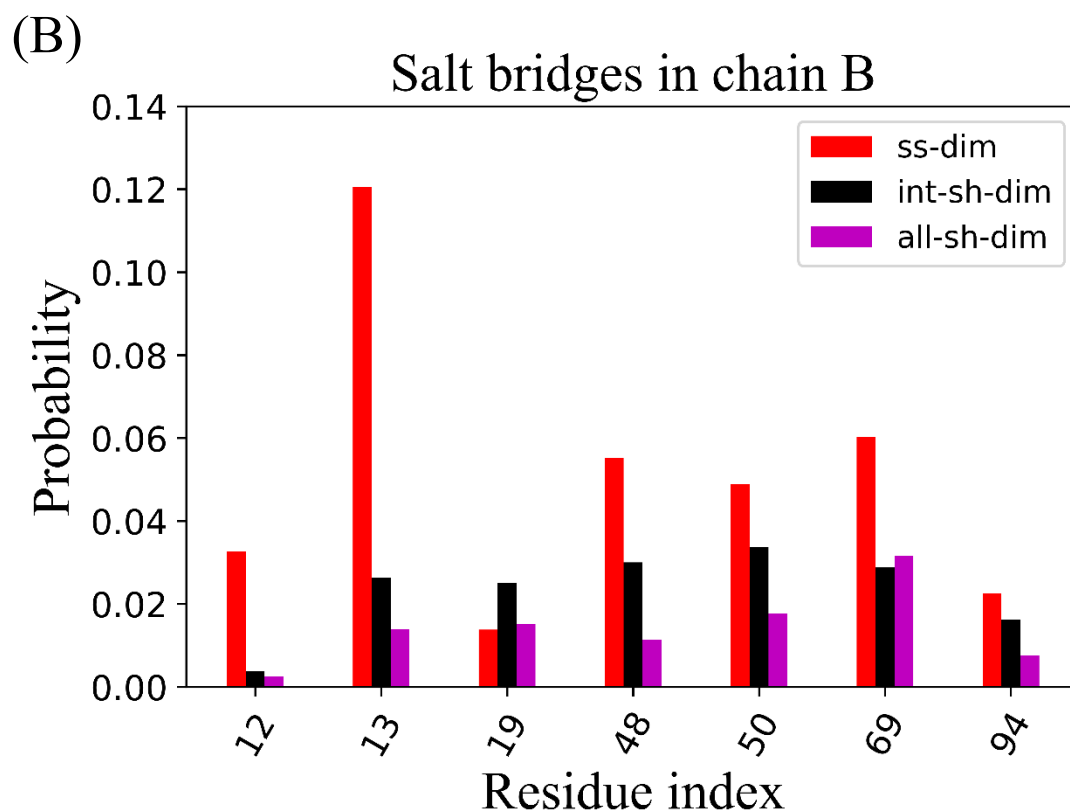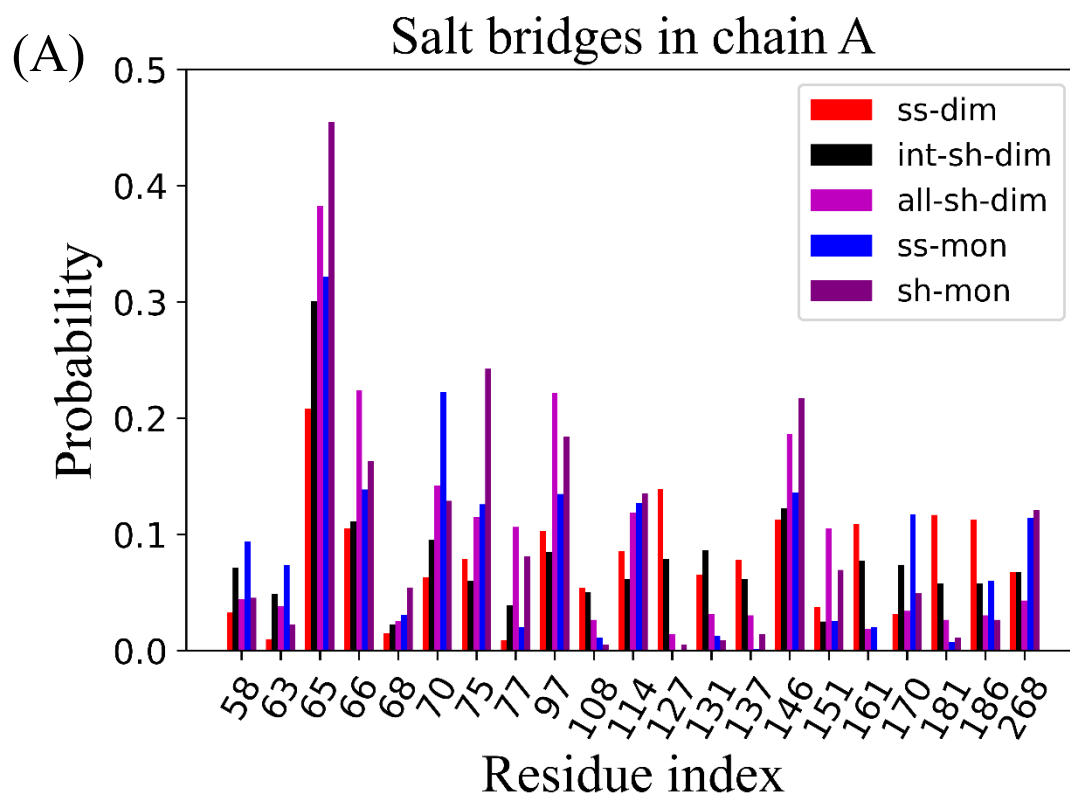
Fig. S10. The distributions of the binding sites on HLA-A forming in salt bridges with ORF8. (A) For chain A of HLA-A (B) For chain B of HLA-A.
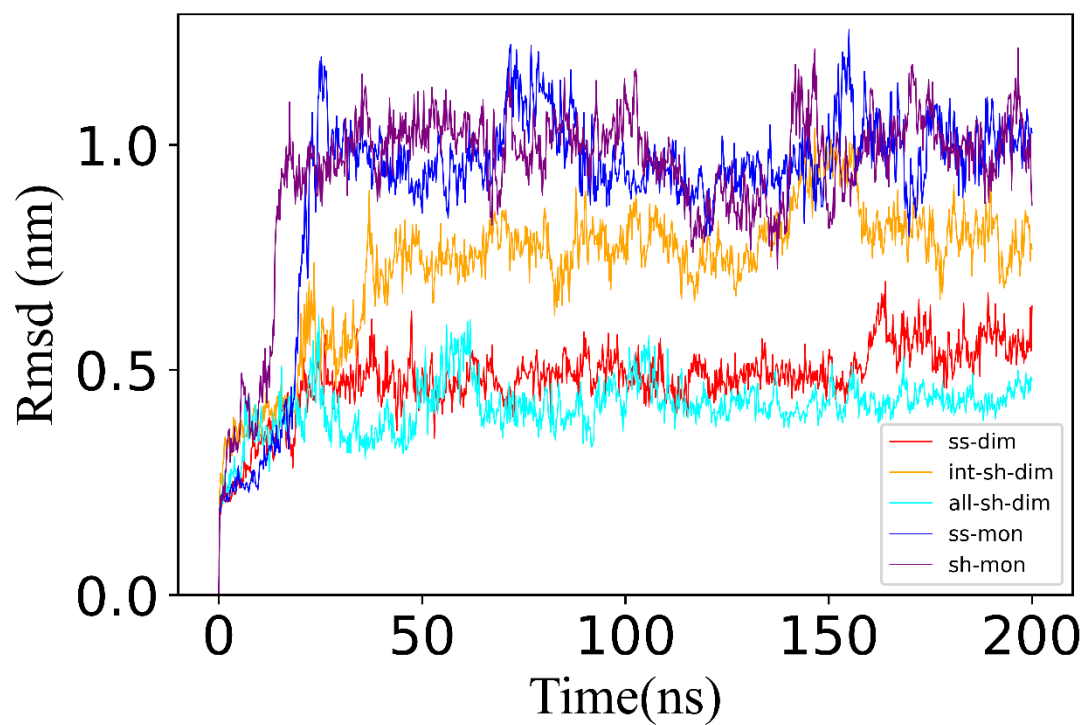
Fig. S11. The curves of the RMSD evolution for the MD simulations on the ORF8-HLA-A complexes with ORF8 in five different states.